Electronic Supplementary Material (ESI) for Catalysis Science & Technology.

MoO_3-modified SAPO-34 for Photocatalytic Nonoxidative Coupling of Methane

Lihan Pan†, Shiqun Wu†, Zhan Huang†, Shengwei Zhang†, Lingzhi Wang†,*, Jinlong Zhang†,*

†Key Lab for Advanced Materials and Joint International Research Laboratory of Precision Chemistry and Molecular Engineering, Feringa Nobel Prize Scientist Joint Research Center, Shanghai Engineering Research Center for Multi-Media Environmental Catalysis and Resource Utilization, Institute of Fine Chemicals, School of Chemistry and Molecular Engineering, East China University of Science & Technology, 130 Meilong Road, Shanghai, 200237, China

Table S1. Elemental analysis of the catalysts.[a]

Samples	Mo (wt%)
1% Mo/SAPO-34	0.74
2% Mo/SAPO-34	1.1
5% Mo/SAPO-34	2.6
10% Mo/SAPO-34	6.1

[a] Analyzed by the ICP-AES method.

Table S2. Results of various samples in different temperature for photo-driven methane NOCM conversion.[a]

Entry	Samples	Reaction Temperature	Conversion [CH_4(%)]	Yield (μmol)		Rate (μmol g^{-1} h^{-1})	Selectivity [C_2H_6(%)]
				C_2H_6	H_2		
1	SAPO-34	298 K	0.684	0.1680	2.3094	0.3490	97.45
2	1%Mo/SAPO-34	298 K	0.949	0.2263	3.3150	0.4841	93.15
3	2%Mo/SAPO-34	298 K	1.758	0.4279	2.2821	0.8962	97.10
4	5%Mo/SAPO-34	298 K	1.764	0.4498	1.4998	0.8997	100
5	10%Mo/SAPO-34	298 K	0.694	0.1769	0.1561	0.3537	100
6	MoO_3	298 K	0	0	0	0	0
7[b]	5%Mo/SAPO-34	373 K	3.282	0.7139	4.3769	1.6740	90.12
8[c]	5%Mo/SAPO-34	473 K	8.038	1.7563	6.1838	4.1004	90.38

[a] Reaction conditions were as follows: samples, 0.2 g; reaction time, 4 h; reactant, 44.6 μmol of methane; light source, 300 W Xe lamp; reaction temperature, 298 K; quartz reactor, 45 cm^3. The products were collected directly, then analyzed by gas chromatography with flame-ionization and thermal conductivity detector. [b] Reaction conditions are the same as others, except the reaction temperature is 373 K. [c] Reaction conditions are the same as others, except the reaction temperature is 473 K.

Table S3. Representative works on photocatalytic or thermocatalytic non-oxidative reaction of methane.

Samples	Conditions	Rate of methane	Main Products	References
(Zn^{+},Zn^{2+})-ZSM-5-	150 W high-pressure Hg lamp for 8 h; 1 g sample; 200 μmol CH_4	9.80 μmol g^{-1} h^{-1}	Ethane (C_2H_6)	1
Au/m-ZnO-4.8	300 W Xe lamp for 4 h; 1 mg sample; 22.3 μmol CH_4	23.5 μmol g^{-1} h^{-1}	Ethane (C_2H_6)	2
Ga-ETS-10-0.2	150 W high-pressure Hg lamp for 5 h; 0.2 g sample; 200 μmol CH_4	29.8 μmol g^{-1} h^{-1}	Ethane (C_2H_6)	3
Ga_2O_3-K	300-W Xe lamp for 3 h, 0.2 g sample; 200 μmol CH_4	0.17%	Ethane (C_2H_6)	4
Pt/HGTS (2%)	300 W Xe lamp for 4 h; 0.2 g sample; 44.6 μmol CH_4	3.48 μmol g^{-1} h^{-1}	Ethane (C_2H_6)	5
SiO_2-Al_2O_3	250 W Xe lamp for 18 h; 1.0 g sample; 100 μmol CH_4	0.33 μmol g^{-1} h^{-1}	Ethane (C_2H_6)	6
SiO_2-Al_2O_3-TiO_2 (0.5 mol % of Ti and 10 mol % of Al)	250 W Xe lamp for 6 h; 1.0 g sample; 200 μmol CH_4	1.47 μmol g^{-1} h^{-1}	Ethane (C_2H_6)	7
0.5% Fe©SiO_2	1223 K; fixed-bed microreactor; 90 volume percent (vol %) CH_4/N_2	48%	53% ethene; 25% naphthalene; 22% benzene	8
PdS/ZrO_2	0.5 g sample; 1323 K; flow reactor; 5% CH_4/Ar mixture gas;	18%	ethylene selectivity near 20%	9
5%Mo/ZSM-5/1	0.5 g sample; 973 K for 4h; fixed bed flow quartz; 3600 mL/h g methane	11.3%	Benzene (70%)	10
5%Mo/MCM-22	0.5 g sample; 973 K for 4h; fixed bed flow quartz; 3600 mL/h g methane	6%	Benzene (60%)	10
im-Mo/HZSM-5(H)	0.2 g sample; 973 K; fixed bed flow quartz; 1500 mL/h g 10% N_2/CH_4	2.4 μmol g^{-1} s^{-1}	BTX(benzene, toluene, and xylene) (80%)	11
Fe(5)-Zr(1)-ZSM-5	0.2 g sample; 1023 K for 6h; fixed-bed tubular quartz reactor; 100 sccm of N_2/CH_4 90:10 mixture	1.9%	Benzene (48%) Coke (35.3%)	12
Fe(5)-Mo(1)-ZSM-5	0.2 g sample; 1023 K for 6h; fixed-bed tubular quartz reactor; 100 sccm of N_2/CH_4 90:10 mixture	0.0%	Benzene (4%) Coke (95.3%)	12
10%Mo/HMFI-B	1 g sample; 973 K; fixed bed continuous plug-flow microreactor;	7%	Benzene and naphthalene	13
4.7%Mo/lamellar MWW	0.3g sample; 983 K; fixed bed reactor; 1600 mL gcat-1 h-1 methane	11%	Benzene (90%)	14
3%Mo/Al_2O_3	0.3g sample; 973 K; quartz reactor;	7.4%	Benzene (4%)	15

	1440 mL/g h methane		C_2 (2.1%)	
			Coke (88.9%)	
	1.0g sample; 923 K; fixed-bed		Benzene (72.9)	16
3%Mo/HSAPO-34	continuous-flow quartz microreactor;	0.6%	C_2 (10.1)	
	1600 mL/g h methane			
Mo/SAPO-34	300 W Xe lamp for 4 h; 0.2 g sample;	8.04%	Ethane	This
	44.6 μmol CH_4 473K	4.10μmol g^{-1} h^{-1}	(C_2H_6)	work

Table S4. The Mo^{5+}/Mo^{6+} and $Mo^{5+}/(Mo^{5+}+Mo^{6+})$ with the different loading.[a]

Samples	Mo^{5+}/Mo^{6+}	$Mo^{5+}/(Mo^{5+}+Mo^{6+})$
1% Mo/SAPO-34	0.406	0.278
2% Mo/SAPO-34	0.614	0.381
5% Mo/SAPO-34	0.577	0.366
10% Mo/SAPO-34	0.427	0.299

[a] The ratio of the Mo^{5+} and Mo^{6+} was calculated by area ratio, which denotes the integration of corresponding peaks of XPS date.

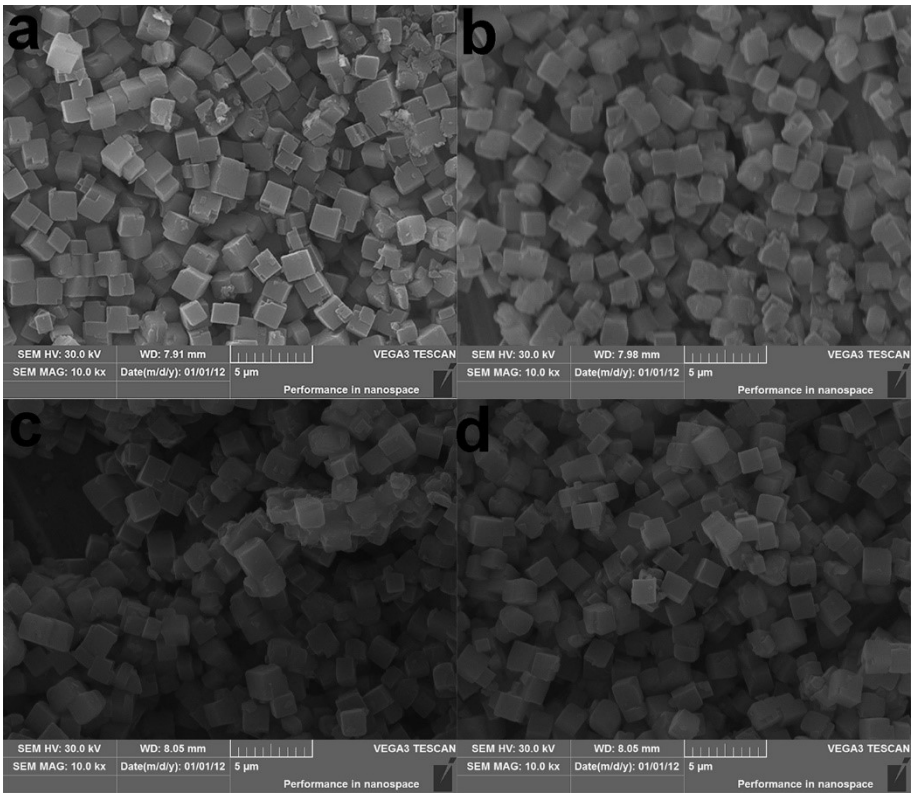

Figure S1. SEM images of (a) SAPO-34, (b) 1% Mo/SAPO-34, (c) 2% Mo/SAPO-34 and (d) 5% Mo/SAPO-34.

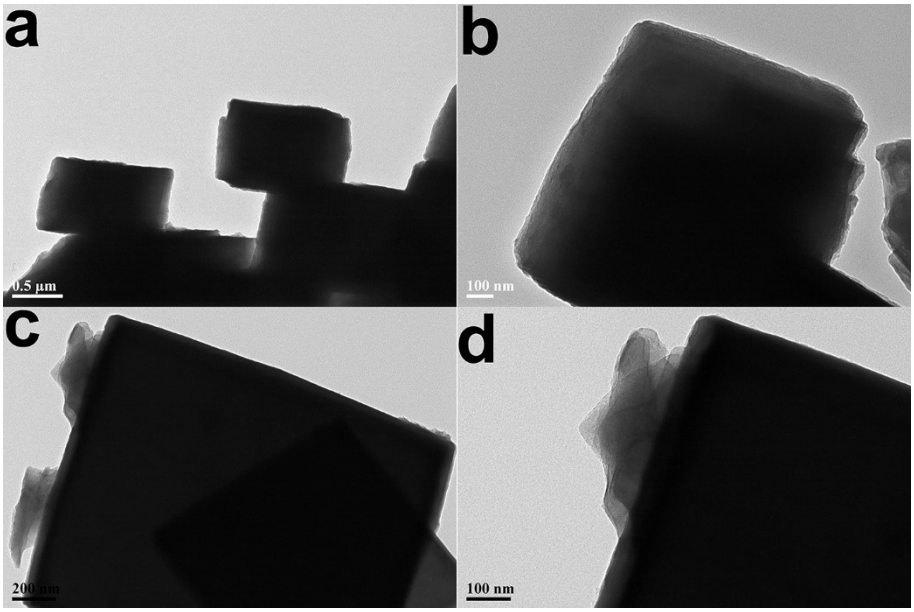

Figure S2. TEM images of 1% Mo/SAPO-34 with different scale bar: (a) 500 nm and (b) 100 nm; 5% Mo/SAPO-34 with different scale bar: (c) 200 nm and (d) 100 nm.

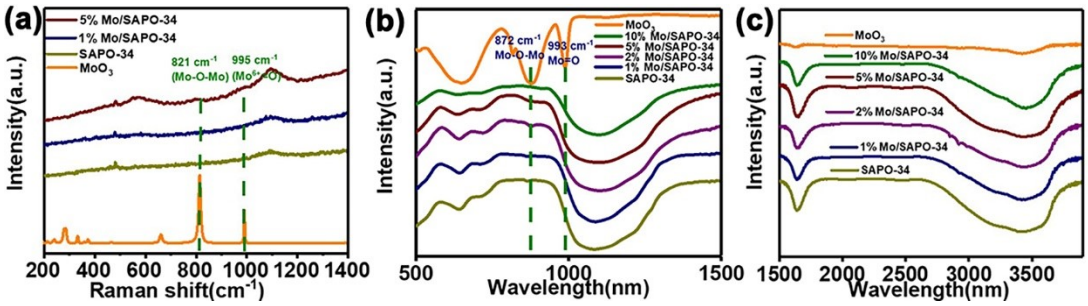

Figure S3. (a) The Raman spectrum, (b) and (c) FTIR spectra of SAPO-34, Mo-SAPO-34 (1%, 2%, 5%, 10%) and MoO_3, respectively.

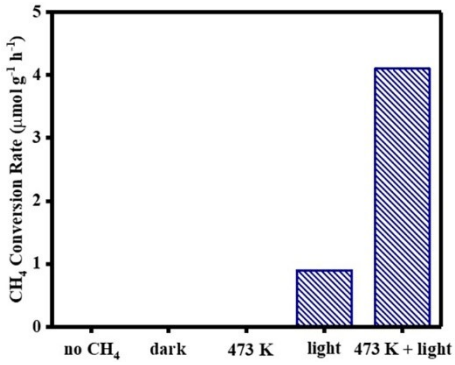

Figure S4. Comparison of experiment condition. The detected conversion of methane with different reaction conditions, conditions from left to right: 0.2 g catalyst with Xe lamp irradiation in a vacuum; 0.2 g catalyst and 1 mL methane without light; 0.2 g catalyst and 1 mL methane heating at 473 K without light for 4 h; 0.2 g catalyst and 1ml methane with Xe lamp irradiation for 4 h; 0.2 g catalyst and 1ml methane heating at 473 K with Xe lamp irradiation for 4 h.

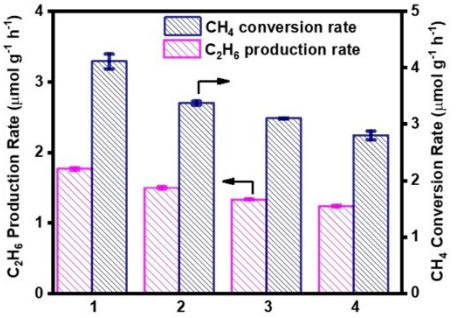

Figure S5. The cycle experiments of Mo/SAPO-34 (5%).

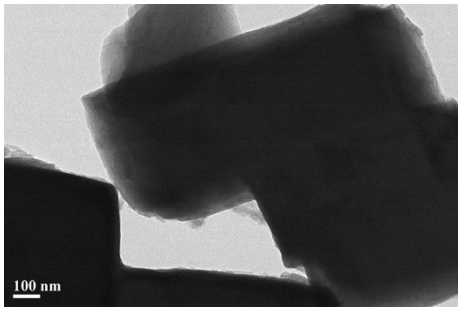

Figure S6. TEM images of recycle 5% Mo/SAPO-34.

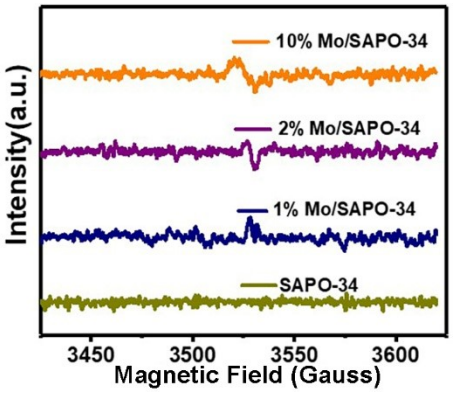

Figure S7. The EPR results of different Mo content of SAPO-34 (0%, 1%, 2% 10%).

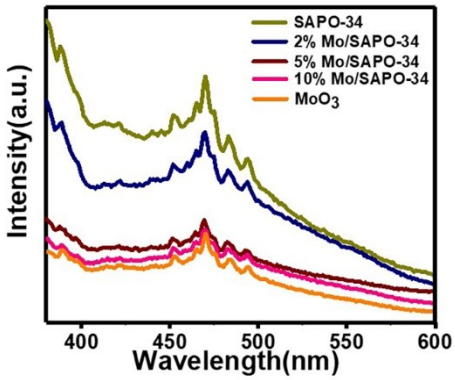

Figure S8. Room-temperature photoluminescence (PL) emission spectra of different samples.

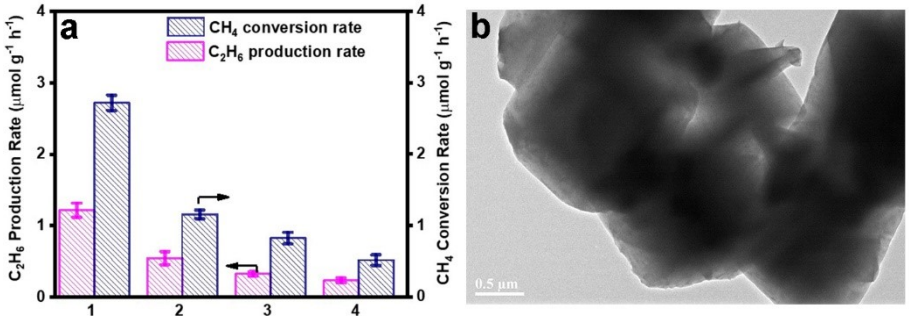

Figure S9. (a)The recycle experiments of 2% Mo/SAPO-34; (b) TEM images of recycle 2% Mo/SAPO-34.

References:

[1] Li, L.; Li, G. D.; Yan, C.; Mu, X. Y.; Pan, X. L.; Zou, X. X.; Wang, K. X.; Chen, J. S. Efficient Sunlight-Driven Dehydrogenative Coupling of Methane to Ethane over a Zn^{+}-Modified Zeolite. Angew. Chem. Int. Ed. **2011**, *50*, 8299-8303.

[2] Meng, L.; Chen, Z.; Ma, Z.; He, S.; Hou, Y.; Li, H.; Yuan, R.; Huang, X.; Wang, X.; Wang, X.; Long, J. Gold Plasmon-induced Photocatalytic Dehydrogenative Coupling of Methane to Ethane on Polar Oxide Surfaces. Energy Environ. Sci. **2018**, *11*, 294-298.

[3] Li, L.; Cai, Y. Y.; Li, G. D.; Mu, X. Y.; Wang, K. X.; Chen, J. S. Synergistic Effect on the Photoactivation of the Methane C-H Bond over Ga^{3+}-Modified ETS-10. Angew. Chem. Int. Ed. **2012**, *51*, 4702-4706.

[4] Yuliati, L.; Hattori, T.; Itoh, H.; Yoshida, H., Photocatalytic nonoxidative coupling of methane on gallium oxide and silica-supported gallium oxide. Journal of Catalysis 2008, 257 (2), 396-402.

[5] Wu, S.; Tan, X.; Lei, J.; Chen, H.; Wang, L.; Zhang, J., Ga-Doped and Pt-Loaded Porous TiO_2–SiO_2 for Photocatalytic Nonoxidative Coupling of Methane. Journal of the American Chemical Society 2019, 141 (16), 6592-6600.

[6] Kato, Y.; Yoshida, H.; Hattori, T. Photoinduced Non-oxidative Coupling of Methane over Silica-alumina and Alumina Around Room Temperature. Chem. Commun. 1998, 21, 2389-2390.

[7] Yoshida, H.; Matsushita, N.; Kato, Y.; Hattori, T. Synergistic Active Sites on SiO_2-Al_2O_3-TiO_2 Photocatalysts for Direct Methane Coupling. J. Phys. Chem. B. 2003, 107, 8355-8362.

[8] Guo, X.; Fang, G.; Li, G.; Ma, H.; Fan, H.; Yu, L.; Ma, C.; Wu, X.; Deng, D.; Wei, M.; Tan, D.; Si, R.; Zhang, S.; Li, J.; Sun, L.; Tang, Z.; Pan, X.; Bao, X., Direct, Nonoxidative Conversion of Methane to Ethylene, Aromatics, and Hydrogen. Science 2014, 344 (6184), 616.

[9] Zhu, Q.; Wegener, S. L.; Xie, C.; Uche, O.; Neurock, M.; Marks, T. J., Sulfur as a selective 'soft' oxidant for catalytic methane conversion probed by experiment and theory. Nature Chemistry 2013, 5 (2), 104-109.

[10] Smiešková, A.; Hudec, P.; Kumar, N.; Salmi, T.; Murzin, D. Y.; Jorík, V., Aromatization of methane on Mo modified zeolites: Influence of the surface and structural properties of the carriers. Applied Catalysis A: General 2010, 377 (1), 83-91

[11] Liu, H.; Bao, X.; Xu, Y., Methane dehydroaromatization under nonoxidative conditions over Mo/HZSM-5 catalysts: Identification and preparation of the Mo active species. Journal of Catalysis 2006, 239 (2), 441-450.

[12] Denardin, F. G.; Perez-Lopez, O. W., Methane dehydroaromatization over Fe-M/ZSM-5 catalysts (M= Zr, Nb, Mo). Microporous and Mesoporous Materials 2020, 295, 109961.

[13] Derouane-Abd Hamid, S. B.; Anderson, J. R.; Schmidt, I.; Bouchy, C.; Jacobsen, C. J. H.; Derouane, E. G., Effect of the activation procedure on the performance of Mo/H-MFI catalysts for the non-oxidative conversion of methane to aromatics. Catalysis Today 2000, 63 (2), 461-469.

[14] Wu, Y.; Emdadi, L.; Wang, Z.; Fan, W.; Liu, D., Textural and catalytic properties of Mo loaded hierarchical meso-/microporous lamellar MFI and MWW zeolites for direct methane conversion. Applied Catalysis A: General 2014, 470, 344-354.

[15] Liu, S.; Wang, L.; Ohnishi, R.; Ichikawa, M., Bifunctional Catalysis of Mo/HZSM-5 in the Dehydroaromatization of Methane to Benzene and Naphthalene XAFS/TG/DTA/MASS/FTIR Characterization and Supporting Effects. Journal of Catalysis 1999, 181 (2), 175-188.

[16] Zhang, C.-L.; Li, S.; Yuan, Y.; Zhang, W.; Wu, T.-H.; Lin, L.-W., Aromatization of methane in the absence of oxygen over Mo-based catalysts supported on different types of zeolites. Catalysis Letters 1998, 56, 207-